A Molecular Dynamics and X-ray Diffraction Study of $MgCl_2$ in Methanol

Y. Tamura*), E. Spohr), and K. Heinziger**

Max-Planck-Insitut für Chemie (Otto-Hahn-Institut), W-6500 Mainz, Germany

G. Pálinkás and I. Bakó

Central Research Institute for Chemistry, Hungarian Academy of Sciences, H-1025 Budapest, Hungary

Computer Experiments / Liquids / Solutions

A recently developed flexible three-site model for methanol was employed to perform a Molecular Dynamics simulation of a 0.6 molal $MgCl_2$ solution. The ion-methanol and ion-ion potential functions were derived from ab initio calculations. The structural properties of the solution are discussed on the basis of radial and angular distribution functions, the orientation of the methanol molecules, and their geometrical arrangement in the solvation shells of the ions. The dynamical properties of the solution are calculated from various autocorrelation functions. Results are presented for the influence of the individual ions on self-diffusion coefficients, hindered translations, and internal vibrations of the methanol molecules. The comparison of calculated X-ray structure and pair correlation functions with those got from a newly performed X-ray measurement on the same solution shows good agreement.

1. Introduction

The methanol molecule is the simplest organic compound that has both hydrophobic and hydrophilic groups and that forms strong hydrogen bonds via the latter groups with other solvent molecules or ions. Although methanol has such an interesting character as a solvent, the number of studies of structural and dynamical properties of methanolic solutions is still small [1].

An X-ray diffraction study of a $MgCl_2$ solution in methanol has been reported for the first time recently [2]. The scattering data were evaluated on the assumption that the methanol molecule consists of only two sites, namely OH and CH_3, because of the small sensitivity of the H atom for X-rays. This treatment is convenient for the comparison of the experimental data with results of simulations with a three-site model for methanol, but the lack of information on the hydrogen atom positions gives only limited information on the structure of the solution. Unfortunately the experimental concentration was almost three times as high as that in the present simulation. The rescaling of the simulated RDFs does not make sense because of a lack of knowledge on the concentration dependence of the various radial distribution functions. In order to have comparable experimental data a new X-ray diffraction measurement on a 0.6 molal $MgCl_2$ has been carried out. A more detailed picture could be deduced from neutron diffraction studies. Unfortunately, up to now such measurements have been performed (by Dore and coworkers) only for pure methanol (see e.g. ref. [3]). A detailed comparison of their data with results of an MD simulation with a six-site model for methanol has been published quite recently [4]. The reason why diffraction methods have seldom been applied to salts in organic solvents is the strongly increasing difficulties arising in the analysis of the experimental structure function with an increasing number of site-site interactions. Therefore, the combined investigation of electrolyte solutions in organic solvents by computer simulation and diffraction measurements provides not only a check of the pair potentials employed in the simulations, as far the structure of the simulated liquid is concerned, but also contributes significantly to the analysis of the experimental structure function.

From a series of IR studies of solutions of electrolytes in methanol at low temperature Strauss and Symons [5] concluded that the Mg^{2+} causes a redshift and the Cl^- a blueshift of the OH-stretching frequency in the methanol molecules of their first solvation shells. While the IR measurements indicate the formation of solvent shared on-pairs only for lithium halide solutions, conductance measurements lead to the conclusion that ion pairs are formed also in alkaline earth chloride solutions in methanol [6].

There is only one computer simulation of ions in methanol reported in the literature. Jorgensen et al. [7] performed Monte Carlo calculations for a Na^+ and a CH_3O^- surrounded by 127 methanol molecules, where a rigid methanol model was employed. Furthermore, an extended RISM analysis on ion association in an NaCl solution in methanol has been published by Hirata and Levy [8].

In order to investigate the effect of ions on the intramolecular properties of methanol a flexible three site model has been developed where the interactions sites are O, H and CH_3 as a whole. It has been demonstrated by the remarkably good agreement between the results of a Molecular Dynamics (MD) simulation and various experimental data that even such a simplified model is able to describe reliably the structural and dynamical properties of liquid methanol [9, 10]. The same model has been employed successfully in the MD simulation of methanol-water mixtures [11] in combination with the BJH model for water [12].

*) Present address: Institute for Molecular Science, Myodaiji, Okazaki 444, Japan.

**) Present address: Institut für theoretische Chemie, Universität, W-7900 Ulm, Germany.

  0005-9021/92/0202/0147 $ 3.50+.25/0

As the next step in this series of investigations an $MgCl_2$ solution has been simulated with this flexible three site model. The results are presented in this paper. They are compared with the corresponding data from a simulation of an aqueous $MgCl_2$ solution with the same number ratio of solute to solvent and the BJH model of water [13].

In the next section the ion-methanol pair potentials, as derived from *ab initio* calculations, are presented together with some details of the simulation. The structures of the solvation shells are discussed on the basis of various radial and angular distribution functions. Self-diffusion coefficients and the spectral densities of hindered translations and intramolecular vibrations, calculated separately for the methanol molecules in the bulk and the first solvation shells of Mg^{2+} and Cl^-, are presented, derived from the simulation with the help of various autocorrelation functions. The results are compared with experimental data and RISM calculations.

2. Pair Potentials and Details of the Simulations

The three-site model given in ref. [9] has been employed in the simulation for the methanol-methanol interaction. It consists of an intra- and intermolecular part and the flexibility of the molecule is rendered by a three-body potential, similar to the BJH model of water. The equilibrium values for r_{OH}, r_{CO}, and α_{COH} are 0.9451 Å, 1.425 Å, and 108.53°, respectively. C denotes synonymously the carbon atom or the methyl group.

The interaction energies for the Mg^{2+}-methanol and Cl^--methanol super molecules were obtained from *ab initio* calculations by use of the HONDO program [14]. DZP basis sets for oxygen and hydrogen atoms were available in the program while those for ions were taken from ref. [15]. We did not use the counterpoise method because the basis set superposition error was estimated to be less than 2% in the resultant interaction energy minimum, which is smaller than the error from the basis set itself. The geometry of the methanol molecule was taken from ref. [16] which gave the lowest energy minimum among all the configurations reported so far. The energy change due to the rotation of the methyl group around its C_{3v} axis is about 5.4 kJ/mol (eclipsed-staggered) for the single molecule, which amounts to only 1.5% of the binding energy of the Mg^{2+}-methanol complex as shown below. A staggered configuration was choosen for the *ab initio* calculations.

The interaction energy for each complex was calculated for several hundred configurations and fitted to the analytical form:

$$V_{i,\mathrm{Me}}(r) = \sum_{\alpha} \frac{z_i z_\alpha e^2}{r} + \frac{A_{i\alpha}}{r^2} + B_{i\alpha}\exp[-C_{i\alpha}r] \qquad (1)$$

where $z_i e$ and $z_\alpha e$ are the charges on the ion i and the atom α of the methanol molecule. The parameters are listed in Table 1. Fig. 1 shows contours of the fitted potential surface for the Mg^{2+}-methanol and Cl^--methanol complexes with the ions in the COH-plane. The minimum for the Mg^{2+}-complex was found to be −350 kJ/mol, about 50 kJ/mol lower than for the Mg^{2+}-water complex [13]. In the case of water the minimum is positioned directly in the anti-dipole direction, while it is found slightly off this direction for methanol. A linear hydrogen bond formation leads to the lowest energy minimum for both Cl^--water and Cl^--methanol complexes. It is found to be −50 kJ/mol for methanol, which is about 10% lower than for water. The ion-ion pair potentials employed here are the same as used for the simulation of the aqueous $MgCl_2$ solution. They were derived from *ab initio* calculations with the contracted GTO basis set, which is of nearly the same quality as the DZP basis set.

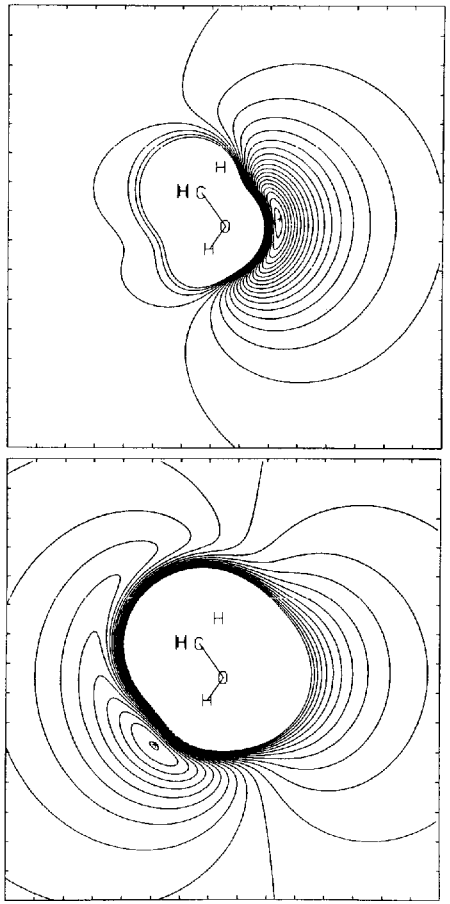

Fig. 1.
Contour plot of the potential energy surface for the Mg^{2+}-methanol (top) and the Cl^--methanol (bottom) complex. The differences between two adjacent contour lines are 20 and 5 kJ/mol with energy minima at −350.26 and −50.35 kJ/mol for Mg^{2+} and Cl^-, respectively

Table 1
Parameters for the non-Coulombic part of the ion-methanol potentials according to Eq. (1)

i	α	$z_i z_\alpha e^2$/kJ Å mol^{-1}	$A_{i\alpha}$/kJ Å^{2}mol^{-1}	$B_{i\alpha}$/kJ mol^{-1}	$C_{i\alpha}$/Å^{-1}
Mg	O	−1667.22	−721.86	4.0778×10^5	4.3937
Mg	H	972.55	−7.2096	4.2904×10^3	0.027485
Mg	C	694.68	232.28	1.8277×10^4	2.6485
Cl	O	833.61	127.00	1.4529×10^5	3.1999
Cl	H	−486.27	−193.37	2.5086×10^4	3.3082
Cl	C	347.34	6.7657	5.9250×10^5	3.2984

In the MD simulation of the 0.6 molal $MgCl_2$ solution the basic cube contained 400 methanol molecules, 8 cations, and 16 anions. The experimental density of 0.8237 g/cm^3 corresponds to a sidelength of 30.14 Å. The Ewald summation was employed for all Coulombic interactions and the shifted force potential method with a cut-of length of 15.07 Å for the non-Coulombic parts of the potential. In order to create the initial configuration a lattice with 8^3 points was constructed and the ions were distributed randomly on these points. Then the 400 methanol molecules were placed randomly on the remaining sites with random orientations. After this manipulation the system was equilibrated during several thousand steps before the collection of data was started. The simulation extended over 5.5 ps with a time step of 0.25 fs. During the simulation the velocities were not rescaled in order to get reliable velocity autocorrelation functions. The average temperature in the whole run was 319 K.

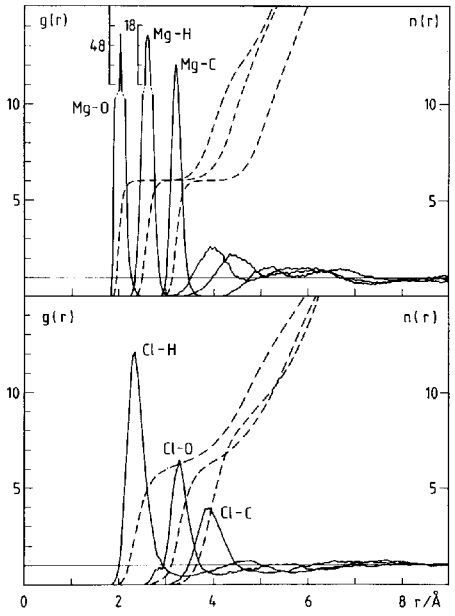

Fig. 2
Ion-oxygen, ion-hydrogen, and ion-carbon radial distribution function and running integration number from an MD simulation of a 0.6 molal $MgCl_2$ solution in methanol

3. Results and Discussion

3.1. Radial Distribution Functions (RDF)

In Fig. 2 the ion-oxygen, ion-hydrogen, and ion-carbon RDFs, $g_{\alpha\beta}(r)$, are drawn together with their corresponding running integration numbers. Characteristic values of the $g_{\alpha\beta}(r)$ and $n_{\alpha\beta}(r)$ are listed in Table 2.

All Mg^{2+}-methanol RDFs show very sharp and well-separated first peaks. The Mg−O nearest neighbor distance is very similar to that found from a simulation of an aqueous $MgCl_2$ solution and slightly smaller than the distance derived from an X-ray investigation (2.07 Å; Ref. [2]). The first peaks in $g_{MgO}(r)$ and $g_{MgH}(r)$ are narrower and about three times as high as in an aqueous solution [13]. These differences can be attributed, at least partly, to the stronger Mg^{2+}-methanol interaction when compared with that of Mg^{2+}-water, as mentioned above. The existence of a well defined first solvation shell is further established by the fact

Table 2
Characteristic values of the radial distribution functions $g_{\alpha\beta}(r)$ for the 0.6 molal $MgCl_2$ solution in methanol[a]

α	β	R_1	r_{M1}	$g_{\alpha\beta}(r_{M1})$	R_2	$n_{\alpha\beta}(R_2)$	r_{m1}	$n_{\alpha\beta}(r_{m1})$	r_{M2}	$g_{\alpha\beta}(r_{M2})$
Mg	O	1.85	2.00	49.3	2.28	5.9	2.5–3.0	6.0	4.0	2.6
Mg	H	2.35	2.61	17.7	2.88	5.9	3.0–3.4	6.0	4.4	2.2
Mg	C	3.00	3.21	12.0	3.48	5.8	3.8–4.2	6.0	5.1	1.5
Cl	O	(2.95)	3.28	6.5	3.72	5.9	4.2	6.6	–	–
Cl	H	2.04	2.35	12.1	2.95	5.9	3.4	6.4	4.7	1.3
Cl	C	3.46	3.85	3.9	4.5	7.8	5.2	9.8	–	–
O	O	2.63	2.83	3.5	3.13	1.9	3.4	2.2	4.7	1.4
O	H	1.70	1.90	2.6	2.15	1.6	2.5	1.8	–	–
O	C	3.23	3.53	2.1	4.43	6.2	4.6	6.7	–	–
H	H	2.15	2.49	2.5	2.99	2.0	3.4	2.5	–	–
H	C	3.00	4.13	1.3	–	–	5.0	8.4	–	–
C	C	3.55	3.90	2.2	5.03	8.6	5.9	12.	7.5	1.2
Mg	Cl	2.5	2.9	8.7	3.4	0.2	3.7	0.3	5.7	≈2

[a] R_i, r_{M_i} and r_{m_i} give the distances in Å, where for the i-th time $g_{\alpha\beta}(r)$ comes to unity, has a maximum and a minimum, respectively. The uncertainty is at least ±0.02 Å. For the methanol-methanol interaction only intermolecular data are given.

that the Mg−O, Mg−H and Mg−C RDFs become zero at the end of the first peak and all three $n(r)$ result in almost exactly six nearest neighbors. Also the existence of a second solvation shell can be inferred from the RDFs. It is again more strongly pronounced than in the aqueous solution but comprises only about seven methanol molecules instead of 15 water molecules. This difference has to be attributed to the fact that only one possibility exists for hydrogen bonding between the methanol molecules in the first and second solvation shell. Similar differences between the hydration and solvation shell as presented here for Mg^{2+} have been found for Na^+ from the MC calculations by Jorgensen et al. [7].

Very similar to Mg^{2+}, the structure of the first solvation shell of Cl^- is much more pronounced in methanol than in water. The explanation for this enhancement is qualitatively the same as given in the preceding paragraph for Mg^{2+}. A second solvation shell around Cl^- cannot be identified in Fig. 2. The running integrations of $g_{ClO}(r)$ and $g_{ClH}(r)$ up to the corresponding first minima, $n(r_{m1})$, result in both cases in a solvation number of 6.5 for the chloride ion. $n_{ClC}(r_{m1})$ gives a larger value than 6.5. This finding is different from Mg^{2+} and indicates an interpenetration of outer molecules into the first solvation shell. It is an interesting feature of the first peaks in the RDFs that their heights decrease significantly in the order Cl−H, Cl−O, and Cl−C while in the aqueous solution the heights for Cl−O and Cl−H were found to be rather similar [13]. The difference might be due to the competition between the two H-atoms of the water molecule in trying to form linear hydrogen bonds with the Cl^- and the rather small energy barrier between these two possible configurations compared with only one potential energy minimum in the methanol case.

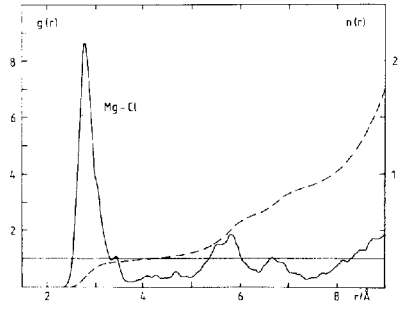

Fig. 3
Mg^{2+} − Cl radial distribution function and running integration number from an MD simulation of a 0.6 molal $MgCl_2$ solution in methanol

The Cl−H, Cl−O, and Cl−C RDFs can be compared with the results of an extended RISM analysis of an NaCl solution in methanol [8]. The positions of the first peaks in g_{ClO} and g_{ClC} resulting from the simulation appear at shorter distances and the peak heights are in all three cases higher than from the RISM analysis. It is not to be expected that these discrepancies have to be attributed to this work as the comparison of the Na−H and Na−C RDFs with simulations by Jorgensen [7] show similar differences.

Ion-ion RDF's are also available, though because of the small number of ions in the sample and the time scale of 5.5 ps of the simulation they are of lower statistical reliability. The RDF's for the like ions do not show any characteristic features and are, therefore not drawn here. The Mg−Cl RDF is shown in Fig. 3. The first sharp peak indicates contact ion pair formation. It can be seen from $n_{MgCl}(r)$ at about 4 Å that one out of four Mg^{2+} forms a contact ion pair. Obviously such an arrangement is rather stable, but one might expect that at significantly longer simulation times it will disappear. The second peak, below 6 Å, points to the existence of solvent shared ion pairs. The probability for their formation seems to be about the same as for contact ion pairs.

3.2. Comparison of MD and X-Ray Data

The experimental technique as well as the details of the data elaboration concerning the newly performed X-ray measurements on the 0.6 molal $MgCl_2$ solution were described before [2]. The experimental distinct structure function was constructed according to the equation:

$$H_d(k) = \frac{I(k) - \sum_\alpha x_\alpha f_\alpha^2(k)}{M(k)}, \tag{2}$$

where $I(k)$ is the normalized intensity, x_α are the mole ratios of the atomic sites, $f_\alpha(k)$ are the X-ray scattering amplitudes and $M(k)$ is a modification function, defined by:

$$M(k) = \left[\sum_\alpha x_\alpha f_\alpha(k)\right]^2. \tag{3}$$

The MD distinct structure function has been calculated as a weighted sum of partial structure functions, $h_{\alpha\beta}(k)$, calculated by Fourier transformation from the site-site RDFs:

$$H_d(k) = \sum_{\alpha,\beta} c_{\alpha\beta}(k) h_{\alpha\beta}(k), \tag{4}$$

with

$$h_{\alpha\beta}(k) = \frac{4\pi\varrho_\beta}{k}\int_0^\infty r\cdot(g_{\alpha\beta}(r) - 1)\sin(kr)\mathrm{d}r, \tag{5}$$

where ϱ_β is the number density of site β. The weighting functions $c_{\alpha\beta}(k)$ were evaluated on the assumption that the system consists of O, H, C, Mg^{2+}, and Cl^- sites by the following equation:

$$c_{\alpha\beta}(k) = \frac{(2-\delta_{\alpha\beta})f_\alpha(k)f_\beta(k)}{M(k)}. \tag{6}$$

The major contributions to the total X-ray structure function result from the O−O,O−C,C−C contributions and the Mg^{2+}−O, Mg^{2+}−C, Cl^-−O, and Cl^-−C interactions.

The total distinct RDFs have been calculated from the distinct structure functions by Fourier transformation:

$$G_d(k) = 1 + \frac{1}{2\pi^2\varrho r}\int_0^\infty k\cdot H_d(k)\sin(kr)\mathrm{d}k. \tag{7}$$

The distinct structure functions and RDFs from the X-ray experiment and the simulation are compared in Figs. 4 and 5, respectively. The comparison of the RDFs shows besides an overall good agreement also some differences. The first resolved peak has to be attributed to Mg^{2+}−O interactions. The experiment leads to a most probable Mg^{2+}−O distance of 2.06 Å which is 0.06 Å larger than the value found from the simulation. The integral over this peak results in an Mg^{2+}−O coordination number of 6 and 6.4 for MD and experiment, respectively. Both differences are hardly outside experimental error and statistical uncertainty of the simulation. The second peak, found at a distance of 2.83 Å, is obviously due to the nearest neighbor O−O interactions, while all the remaining peaks are composite ones.

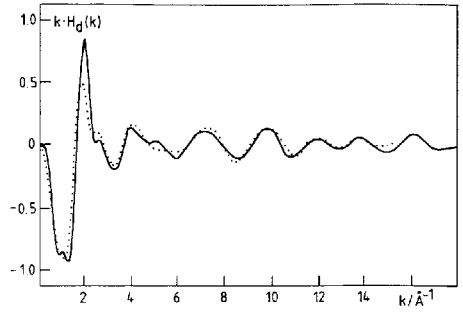

Fig. 4
Distinct structure function for a 0.6 molal $MgCl_2$ solution in methanol from the simulation (full line) and from the X-ray measurement (dots)

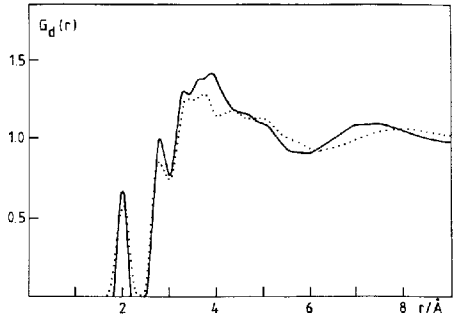

Fig. 5
Intermolecular radial distribution functions for a 0.6 molal $MgCl_2$ solution in methanol from the simulation (full line) and from the X-ray measurement (dots)

The discrepancies between experimental and MD RDFs beyond 3 Å can mainly be attributed to differences in solvent-solvent interactions as can be seen from Fig. 5. In Fig. 6 the ion-solvent and solvent-solvent contributions to the total RDF from the MD simulation are drawn separately. The contribution of the ion-ion interactions is negligible because of their very low weight in the X-ray structure function (see below).

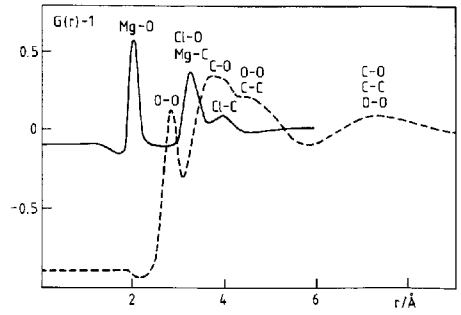

Fig. 6
Ion-solvent (solid line) and solvent-solvent (dashed line) radial distribution functions from the simulation of a 0.6 molal $MgCl_2$ solution in methanol

For a more detailed comparison of experimental and MD data a difference structure function has been introduced by the following equation:

$$\Delta H(k) = H_d(k) - H_{SS}^0(k), \tag{8}$$

where $H_{SS}^0(k)$ is the structure function of the pure solvent H_{pure}, renormalized for the solution density ϱ and the modification function M:

$$H_{SS}^0(k) = \frac{\varrho_0 M^0(k)}{\varrho M(k)} H_{pure}(k). \tag{9}$$

ϱ_0 is the density of pure solvent at the same temperature.

The $H(k)$ difference structure function is composed of all ion-solvent interactions $H_{IS}(k)$ and of a contribution due to changes in solvent-solvent interactions $H_{SS}(k)$ compared to pure solvent:

$$\Delta H(k) = H_{IS}(k) + \Delta H_{SS}(k), \tag{10}$$

where

$$\Delta H_{SS} = H_{SS}(k) - H_{SS}^0(k). \tag{11}$$

The corresponding difference radial distribution function $\Delta G(r)$ calculated by Fourier transformation of $\Delta H(k)$ is given by:

$$\Delta G(r) = G_{IS}(r) + \Delta G_{SS}(r). \tag{12}$$

These $\Delta G(r)$ from experiment and MD simulation, as calculated from corresponding structure functions for the solution and the pure solvent [9, 17], are compared in Fig. 7. The comparison shows good agreement between experimental and MD difference functions in the range of the nearest neighbor distances below 3.3 Å. The assignment for the peaks of difference radial distribution functions in Fig. 7 can be done based in Fig. 6. The first resolved peak in $\Delta G(r)$ is obviously due to $Mg^{2+}-O$ first neighbor interactions. The second peak at distances of 2.75 Å and 2.70 Å for MD and experiment, respectively, represents changes in the H- bonded O–O interactions in solution relative to the pure solvent. This assignment is supported by $\Delta G_{SS}(r)$ as calculated from the MD simulation and shown in Fig. 8.

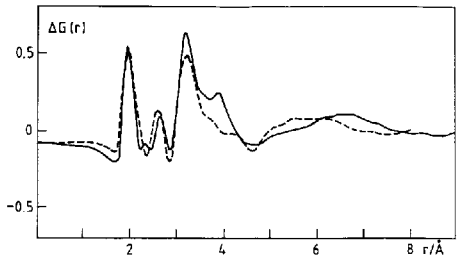

Fig. 7
Difference radial distribution function $\Delta G(r)$ as defined in the text and calculated from the simulation (full line) and an X-ray experiment (dashed line)

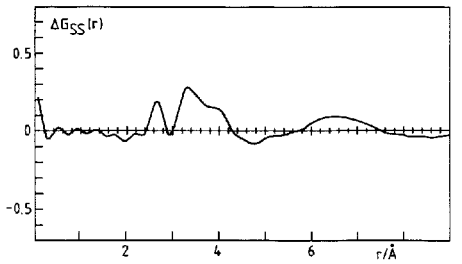

Fig. 8
Difference radial distribution function characterizing the changes in the solvent structure relative to pure solvent as calculated from the MD simulation

The existence of this peak at a distance shorter than the mean nearest neighbor O–O distance shows an increased number of short H-bonds between solvent molecules in the solution. Such shortened hydrogen bonds have also been found in aqueous solutions with Mg^{2+} and other small cations between water molecules in the first and second hydration shell both by X-ray experiments and MD simulations [13, 18]. Discrepancies between experimental and MD difference functions around 4 Å may be due to a more pronounced solvation shell of Mg^{2+} and also to slightly shorter C–O and C–C distances in the model solution. The broad contributions above 5 Å have to be attributed to changes in the second neighbor C–O and C–C interactions in the solution and may be interpreted as a result of solvation shell solvent-solvent interactions absent in pure methanol. Summarizing the results of the comparison between experimental and MD structure as well as radial distribution functions one can conclude that an overal good agreement exists as far as the primary solvation shell of the ions and their effect on the nearest neighbor solvent-solvent interactions are concerned.

3.3 Orientation of the Methanol Molecules

The orientation of the methanol molecules in the first solvation shells of Mg^{2+}- and Cl^- are described by the distributions of $\cos\Phi$ and $\cos\Psi$, respectively. They are shown in Fig. 9 where also Φ and Ψ are defined in the insertions. The distributions demonstrate a strong preference for a trigonal orientation of the methanol molecules surrounding Mg^{2+} and for a linear hydrogen bond formation of the first solvation shell molecules with Cl^-. The preferential orientations are the same as in an aqueous

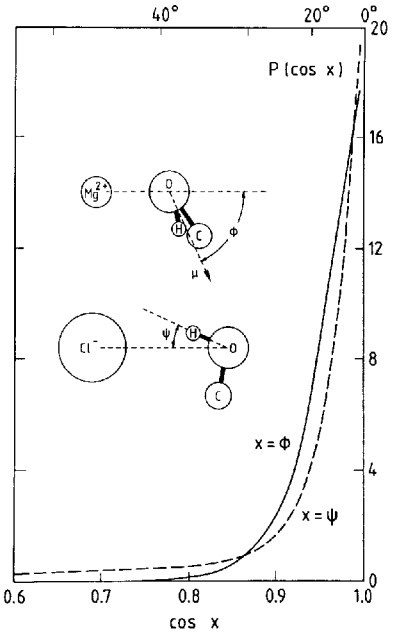

Fig. 9
Distribution of $\cos\Phi$ and $\cos\Psi$ for the methanol molecules in the first solvation shells of Mg^{2+} and Cl^-, respectively; calculated from an MD simulation of a 0.6 molal $MgCl_2$ solution in methanol. μ is the dipole moment vector of the methanol molecule

$MgCl_2$ solution [13], but they are more pronounced here in accordance with the higher and narrower first peaks in the ion-oxygen and ion-hydrogen RDFs, as discussed above.

In Fig. 10 the average values of $\cos(180\text{-}\Phi)$ and $\cos\Psi$ are presented as a function of the Mg–O and Cl–O distance, respectively. $\langle\cos(180\text{-}\Phi)(r)\rangle$ is rather constant (below −0.8) up to about 4.5 Å, which included the first and second solvation shells of Mg^{2+}. Beyond 4.5 Å the preferential orientation slowly decreases without reaching zero even at 9 Å $\langle\cos\Psi(r)\rangle$ is almost one over the range of the first peak in $g_{ClO}(r)$ in agreement with the strong preference for a linear hydrogen bond formation between Cl^- and the methanol molecules in its first solvation shell. The methanol molecules at shorter distances, corresponding to the shoulder in $g_{ClO}(r)$ below 3 Å, show an energetically less favourable orientation. They might belong at the same time to the first solvation shell of Mg^{2+} and Cl^- (solvent shared or contact ion pairs as discussed above) and where Mg^{2+} dominates the orientation. The second peak in $\langle\cos\Psi(r)\rangle$ has no equivalent in $g_{ClO}(r)$. The preferential orientation of the methanol molecules relative to both ions extends significantly further than the one of the water molecules in an aqueous solution of equivalent concentration [13].

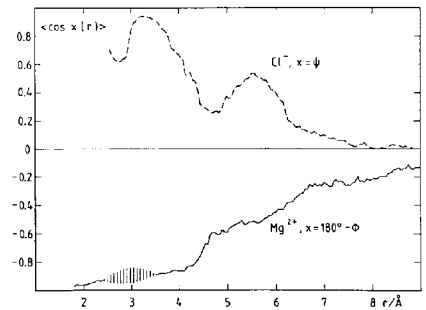

Fig. 10
Average value of $\cos\Psi$ and $\cos(180\text{-}\Phi)$ as a function of ion-oxygen distance, calculated from an MD simulation of a 0.6 molal $MgCl_2$ solution in methanol. Ψ and Φ are defined in the insertion of Fig. 9

3.4. Solvation Shell Structures

The geometrical arrangement of the methanol molecules in the solvation shells of Mg^{2+} and Cl^- has been investigated by calculating the distribution of $\cos\theta$ where θ is defined in the insertion of Fig. 11. The figure shows in addition to $P(\cos\theta)$ the running integration number $n(\cos\theta)$. The conclusion: There exists a well defined octahedral arrangement of the six methanol molecules in the first solvation shell of Mg^{2+} with a rather narrow distribution arround the octahedral sites. The solvation shell of Cl^- shows no symmetry at all. The angles θ are almost uniformly distributed except for the excluded volume effect for $\cos\theta > 0.8$.

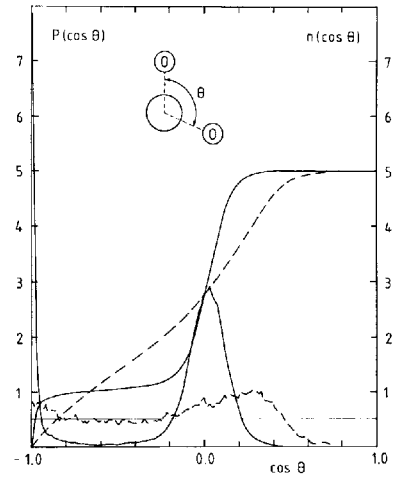

Fig. 11
Distribution and running integration number of $\cos\theta$ – where θ is defined as the oxygen-ion-oxygen angle – calculated for the six methanol molecules in the first solvation shells of Mg^{2+} (full) and Cl (dashed), from an MD simulation of a 0.6 molal $MgCl_2$ solution in methanol

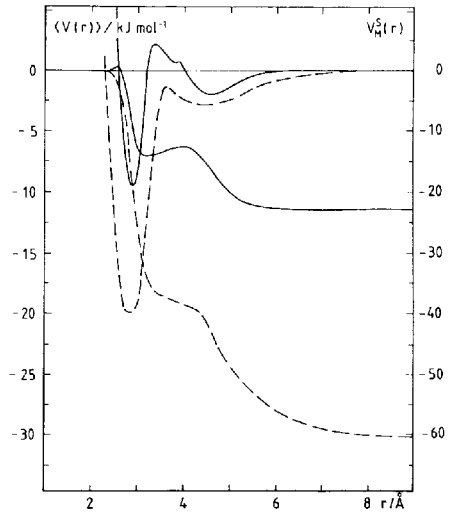

Fig. 12
Average potential energy of two methanol molecules as a function of their O–O distance and running integrated interaction energies according to Eq. (13) for the methanol molecules in a 0.6 molal $MgCl_2$ solution (full) and in pure methanol (dashed)

3.5. Interaction Energies

The average potential energy of two methanol molecules as a function of the O–O distance, $\langle V_{MM}(r)\rangle$, and of a methanol molecule in the field of an Mg^{2+} and Cl as a function of ion-oxygen distance $\langle V_{IonM}(r)\rangle$, are presented in Figs. 12 and 13, respectively. The integrated interaction energies as defined by:

$$V_\alpha^S(r) = 4\pi\varrho_m \int_0^r g_{\alpha O}(r')\langle V_{\alpha M}(r')\rangle r'^2 dr' \qquad (13)$$

are drawn additionally. ϱ_m is the number density of the methanol molecules and α denotes either a methanol molecule or one of the ions.

In order to investigate the influence of the ions on the interaction energies between two methanol molecules $\langle V_{MM}(r)\rangle$ and $V_M^S(r)$ for the 0.6 molal $MgCl_2$ solution are compared in Fig. 12 with those of pure methanol [9]. The comparison demonstrates that the ions strongly disturb the hydrogen bond formation of methanol. The reduction of the minimum in $\langle V_{MM}(r)\rangle$ by a factor of more than two results mainly from the interactions between the methanol molecules in the first solvation shell of Mg^{2+}. They are forced into energetically unfavorable orientations orientations relative to each other by the strong influence of the Mg^{+2}. Their O–O distances in the octahedral symmetry are 2.83 Å, which is about the same distance as for the methanol dimer. The positive interaction energies in the distance range 3.3–4 Å seem to result from the combined effect of both ions on the relative orientation of two methanol molecules as it can occur near ion pairs and solvent shared ion pairs. A second minimum in $\langle V_{MM}(r)\rangle$ exists around 4.6 Å which almost coincides with the second peak in $g_{oo}(r)$ and indicates energetically preferential orientation of methanol molecules relative to each other up to distances of 6 Å. The disappearance of the long range order in methanol by addition of $MgCl_2$ becomes evident also from $V_M^S(r)$, which is at 9 Å almost three times as large in pure methanol as in the solution.

The average potential energies of the methanol molecules in the field of Mg^{2+} and Cl^- and their integrated interaction energies are shown in Fig. 13. While the energy minimum in the chloride case appears at the same distance as the maximum of the Cl–O RDF, in the Mg^{2+} case it is positioned slightly below that point. In the Cl case the minimum is about 10% less deep than the pair potential minimum as a consequence of thermal motions and the interactions with other neighboring methanol molecules. Unlike Cl^- the minimum in $\langle V_{MgM}(r)\rangle$ is deeper than the pair potential minimum. In spite of the same effects being active as in the chloride case they are overcompensated by the strong effect of the Mg^{2+} on the intramolecular geometry of the methanol molecules (Table 3 and discussion below), which results in an increase of the dipole moment and consequently a more negative pair interaction energy relative to the *ab initio* calculations where the gas phase geometry was employed. The curves for $V_\alpha^S(r)$ show that for Mg^{2+} the first solvation shell is energetically well defined and a second one is indicated, while for Cl^- even the first shell is not very pronounced. The far ranging preferential orientation of the methanol relative to the ions, as demonstrated in Fig. 10, is also reflected in $\langle V_{\alpha M}(r)\rangle$ which even at 9 Å is different from zero. Consequently $V_\alpha^S(r)$ has not reached its limiting value at that distance.

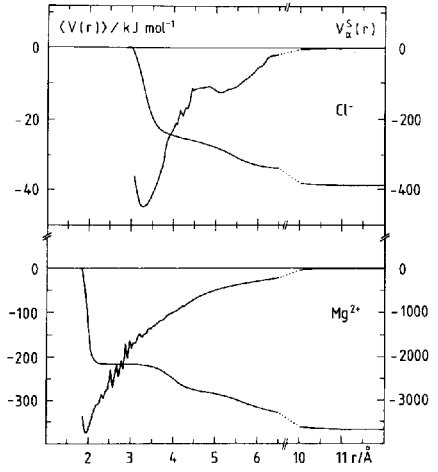

Fig. 13
Average potential energy of a methanol molecule in the field of a chloride ion (top) and a magnesium ion (bottom) together with the running integrated interaction energies according to Eq. (13) calculated from a simulation of a 0.6 molal $MgCl_2$ solution in methanol

Table 3
Average values of bond lengths, bond angles, and dipole moments for the methanol molecules in the bulk and in the first solvation shells of the ions

	R_{OH}/Å	R_{CO}/Å	R_{CH}/Å	α_{COH}/deg.	μ/D
bulk	0.966	1.427	1.939	106.7	1.99
Mg^{2+}	0.981	1.434	1.918	103.6	2.09
Cl^-	0.965	1.426	1.937	106.7	1.99

This strong effect of the ions on the methanol-methanol interactions is demonstrated additionally by the comparison of the pair interaction energy distributions which are shown on Fig. 14 for the $MgCl_2$ solution and pure methanol. The maximum which appears in pure methanol at about 22 kJ/mol is strongly reduced in the solution and shifted to slighly less negative energies in accordance with $\langle V_{MM}(r)\rangle$ in Fig. 12. Even more impressive are the changes for positive interaction energies, the number of which is strongly increased in the solution.

The ion-methanol pair interaction energy distributions are shown in Fig. 15. Again there are two peaks for Mg^{2+}, reflecting the two solvation shells (Fig. 2). For the first shell, the maximum is positioned at about −365 kJ/mol in accordance with the minimum in $\langle V_{MgM}(r)\rangle$. The peak is very

narrow in keeping with a rather narrow distribution of the orientations as shown in Fig. 9. The maximum corresponding to the second shell appears at about −100 kJ/mol and is broader. While for Cl^- only one maximum at negative energies can be seen with an energy slightly below −50 kJ/mol (in accordance with Fig. 13) there is a strong increase at the positive energy side with a shoulder at about 25 kJ/mol. These positive energies seem to result from methanol molecules which belong at the same time to the solvation shell of Mg^{2+} and Cl^- and where the strong effect of Mg^{2+} forces the molecule into an energetically unfavorable orientation relative to Cl^-.

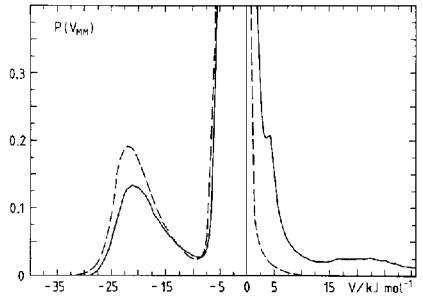

Fig. 14
Normalized distributions of pair interaction energies for methanol-methanol from simulations of a 0.6 $MgCl_2$ solution (full) and pure methanol (dashed)

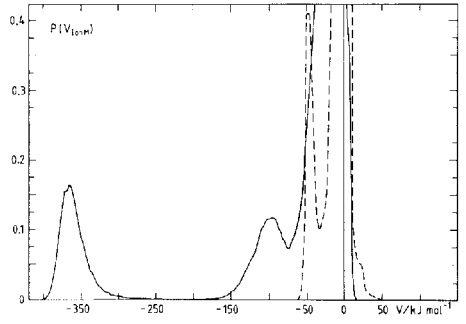

Fig. 15
Normalized pair interaction energy distributions for Mg^{2+}-methanol (full) and Cl^--methanol (dashed) from a simulation of a 0.6 molal $MgCl_2$ solution

The effects of $MgCl_2$ on the structure of liquid methanol as presented here are significantly stronger than on water as can be seen from the comparsion with the simulation on an aqueous $MgCl_2$ solution [13].

3.6. Self-Diffusion Coefficients

The self-diffusion coefficients have been derived from the velocity autocorrelation functions with the help of the Green-Kubo relation:

$$D = \lim_{t\to\infty} \frac{1}{3}\int_0^t \langle \boldsymbol{v}(0)\cdot\boldsymbol{v}(t')\rangle dt', \qquad (14)$$

where the averages are calculated according to:

$$\langle \boldsymbol{v}(0)\cdot\boldsymbol{v}(t)\rangle = \frac{1}{N_T N}\sum_{i=1}^{N_T}\sum_{j=1}^{N} \boldsymbol{v}_j(t_i)\cdot\boldsymbol{v}_j(t_j+t), \qquad (15)$$

and where N denotes the number of particles, N_T the number of time averages, and $\boldsymbol{v}_j(t)$ the velocity of particle j at time t.

The normalized velocity autocorrelation functions for the ions and for the center of mass of all methanol molecules in the 0.6 molal $MgCl_2$ solution are shown in Fig. 16. In addition, they have been calculated separately for three methanol subsystems in the solution, namely bulk methanol and the mathanol molecules in the first solvation shells of Mg^{2+} and Cl , in order to study in single ion effect on the translational motions of methanol. They are depicted in Fig. 17. The first solvation shells are assumed to extend to the first minima in the corresponding ion-oxygen RDFs. For a better comparison of their different time dependences the acf's are drawn only up to 1.2 ps while a correlation time of 2.5 ps is used in all cases for the evaluation of the self-diffusion coefficients. They are found to be (2.2 ± 0.2), (0.6 ± 0.2), and $(2.0\pm0.2)\cdot10^{-5}$ cm²/s for the methanol, Mg^{2+}, and Cl^-, respectively. The self-diffusion coefficients for the three methanol subsystems have been calculated to be (2.4 ± 0.2), (0.5 ± 0.2), and $(2.0\pm0.2)\cdot10^{-5}$ cm²/s for bulk methanol, solvation shell of Mg^{2+} and Cl^-, respectively.

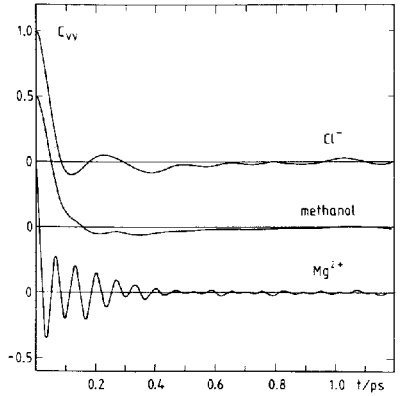

Fig. 16
Normalized velocity autocorrelation functions $\langle \boldsymbol{v}(0)\cdot\boldsymbol{v}(t)\rangle/\langle \boldsymbol{v}(0)^2\rangle$ for the methanol molecules (center of mass), the magnesium ions, and the chloride ions, calculated from an MD simulation of a 0.6 molal $MgCl_2$ solution in methanol

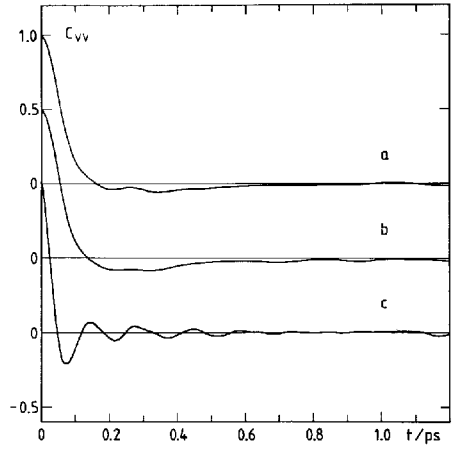

Fig. 17
Normalized velocity autocorrelation functions for the methanol molecules (center of mass) calculated from an MD simulation of a 0.6 molal $MgCl_2$ solution separately for bulk methanol (a) and the methanol molecules in the first solvation shells of Cl^- (b) and Mg^{2+} (c)

Experimental self-diffusion coefficients for Mg^{2+} in methanol could not be found in the literature. The very low value for Mg^{2+}, which is similar to the ones for Sr^{2+} and Li^+ in water [19, 20], is a consequence of its strong interactions with the solvent molecules in the first solvation shells as can be seen from the spectral densities of the hindered translational motions of Mg^{2+} discussed in the next section. This is, furthermore, confirmed by the self-diffusion coefficient of the methanol molecules in the first solvation shell of Mg^{2+} which is in the limits of uncertainty the same as for the ion itself (see above).

The self-diffusion coefficient of Cl^- in methanol has been measured by Hawlicka [21]. In a 0.01 molal NaCl solution a value of $1.4 \cdot 10^{-5}$ cm^2/s has been found for a temperature of 298 K. As its concentration dependence has been determined only for concentrations up to 0.01 molar and the temperature dependence is not known, a direct comparison with the value from the simulation is not possible. As the self-diffusion coefficient tends to decrease with increasing concentration and to increase with increasing temperature both effects will at least partly cancel. If in addition the relatively large statistical uncertainty is taken into account the simulated value seems to be quite reasonable.

The self-diffusion coefficients of Cl^- and of the methanol molecules in its first solvation shell are found to be nearly the same and only about 20% lower than that of bulk methanol. The value for Cl^- calculated from simulations of various aqueous electrolyte solutions in only about half of that found here [19].

The self-diffusion coefficient for all methanol molecules in the solution (the only one which is directly accessible by experiment) is significantly smaller than the one calculated from a simulation of pure methanol with the same model ($2.6 \cdot 10^{-5}$ cm^2/s at 286 K [9]). This result agree qualitatively with measurements on NaI solutions in methanol by Hawlicka [22], where a strong decrease was found with an increase in NaI concentration, when the temperature dependence of the self-diffusion coefficient of methanol is taken into account [23].

3.7. Hindered Translations

The spectral densities of the hindered translational motions have been calculated by Fourier transformation:

$$f(\omega) = \int_0^\infty \frac{\langle v(0) \cdot v(t) \rangle}{\langle v(0)^2 \rangle} \cos(\omega t) \mathrm{d}t \qquad (16)$$

from the normalized velocity autocorrelation functions as shown in Figs. 16 and 17 and are presented for Mg^{2+} and Cl^- in Fig. 18 and separately for the three methanol subsystems in Fig. 19.

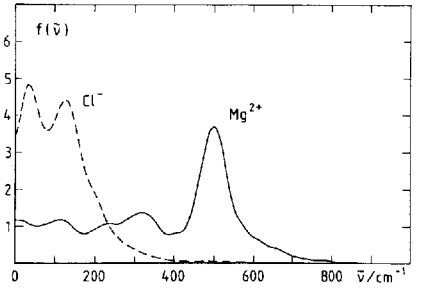

Fig. 18
Spectral densities of the hindered translations of the magnesium ion (full) and the chloride ion (dashed) calculated from an MD simulation of a 0.6 molal $MgCl_2$ solution in methanol and given in arbitrary units

The Cl^- spectrum consists of a double peak with maxima at about 30 and 125 cm^{-1} (Fig. 18). In accordance with the assignment in the case of the aqueous solution [19], the low frequency peak may be attributed to the motion of the bare Cl^- while the stronger interactions of Cl^- with its neighborhood – when engaged in contact or solvent shared ion pairs – lead to the peak at higher frequency.

The Mg^{2+} spectrum shows a single peak at about 500 cm^{-1} (Fig. 18). This high frequency for the hindered translation is expected from the velocity autocorrelation function (Fig. 16) and results from the motions of Mg^{2+} in the cage of the firmly attached six methanol molecules in its first solvation shell. This assignment explains also the small self-diffusion coefficient as it means that the ion can move only together with its six solvation shell molecules and this complex is further hindered by hydrogen bond formation between first and second solvation shell.

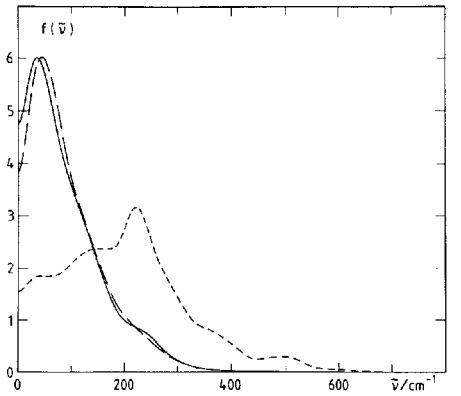

Fig. 19
Spectral densities of the hindered translations of the methanol molecules (in arbitrary units) calculated from an MD simulation of a 0.6 molal $MgCl_2$ solution separately for bulk methanol (full) and the methanol molecules in the first solvation shells of Cl^- (– – –) and Mg^{2+} (------)

The spectrum of the hindered translations of bulk methanol shows a single peak at about 35 cm^{-1} (Fig. 19). As expected from the similarities in the velocity autocorrelation functions depicted in Fig. 17 this spectrum is almost identical with that for the methanol molecules in the first solvation shell of Cl^-, except for a blueshift of the peak maximum by about 10 cm^{-1}. The strong interaction between Mg^{2+} and its first solvation shell causes not only a high frequency motion of Mg^{2+}, as shown in Fig. 18, but effects also strongly the hindered translations of its solvation shell molecules, resulting in a maximum around 225 cm^{-1}.

3.8. Intramolecular Geometry and Vibrations

It has been demonstrated in a preceding paper [9] that the methanol model exployed in this simulation describes correctly the gas-liquid frequency shift of the intramolecular vibrations. The change of the intramolecular O–H distance on condensation corresponds to this shift according to the empirical proportionality factor between the O–H stretching frequency and the O–H distance of 20000 cm^{-1}/Å [24]. As the model describes correctly the intramolecular changes upon hydrogen bond formation it is expected that the effect of the ions on the intramolecular properties of methanol can also be calculated reliably from the simulation.

In order to calculate the single ion effect on the intramolecular geometry and the vibrations, the 400 methanol molecules in the solution are divided again into the three subsystems described above. The average values of the bond lengths and the bond angles are given in Table 3. The total spectral densitites of the vibrational motions have been calculated separately for the three subsystems as the weighted sum of the Fourier transforms of the normalized velocity autocorrelation functions of the three sites in the methanol molecule. The results are shown in Fig. 20 and the positions of the peak maxima are listed in Table 4.

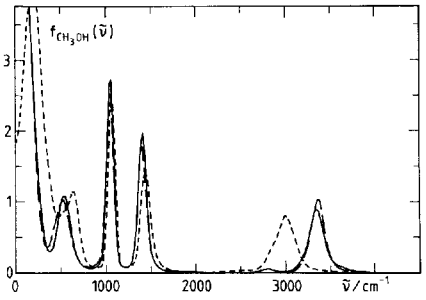

Fig. 20
Total spectral densities of liquid methanol (in arbitrary units) calculated separately for the molecules in the bulk (full) and in the first solvation shells of Cl^- (– – –) and Mg^{2+} (-------) from an MD simulation of a 0.6 molal $MgCl_2$ solution in methanol

Table 4
Frequencies, in cm^{-1}, of the peak maxima in the total spectral densities of methanol calculated separately for the molecules in the bulk and in the first solvation shells of Mg^{2+} and Cl^- [a]

	bulk methanol	first solvation shell of anion	first solvation shell of cation
libration	534	522	628
CO stretch	1045	1045	1064
COH bend	1406	1404	1440
OH stretch	3344	3368	2997

[a] The statistical uncertainty of the peak positions is estimated to be ±10 cm^{-1}.

The frequencies found for bulk methanol do not differ significantly from those of pure methanol. Between bulk methanol and methanol in the first solvation shell of Cl^- a small difference outside of statistical uncertainty has been found only for O–H stretching frequency. Such a small difference might not be considered really significant if there were no strong indications for a blueshift caused by Cl^- from IR measurements of LiCl and $MgCl_2$ solutions at a temperature of −125 °C by Strauss and Symons [5]. The difference between the experimental blueshift of 100 cm^{-1} and the 24 cm^{-1} calculated from the simulation may have to be attributed, at least partly, to the low temperature at which the experiments were performed. Further indications for such an effect result from Raman measurements of LiCl solutions in ethanol by Yamauchi and Kanno [25] at liquid nitrogen temperatures who attributed a blueshift of similar size (100 cm^{-1}) to the Cl^--ethanol interactions.

The Mg^{2+} causes a blueshift of the librational, the C–O stretching and the COH bending frequencies and a strong redshift of the O–H stretching frequency for the methanol molecules of its first solvation shell relative to bulk methanol (Fig. 20 and Table 4). The frequencies of the peak maxima

for the hindered translations are below 300 cm^{-1}. The bands due to translational motion of methanol molecules in the first hydration shell of Cl^- and in the bulk are not resolved, while the strong interactions of Mg^{2+} with its solvation shell molecules leads to a well resolved band at about 225 cm^{-1}. The blueshift of the librational frequencies and the bending vibration seem to be significant while the one of the C–O stretching vibration is hardly outside the limits of statistical uncertainty. There is no information from experiments on ion induced frequency shifts in the range below 2000 cm^{-1}.

The redshift of the O–H stretching frequency of methanol caused by Mg^{2+} is of similar size as the shifts which result from the interactions of Ca^{2+} and Li^+ with the water molecules in their first hydration shells [26, 27]. In the case of water these predictions of a strong cation effect on the O–H stretching vibrations by the simulations have recently been confirmed experimentally for several divalent cations [28]. Strauss and Symons concluded from their IR measurements of pure methanol and of a 1.2 molal $MgCl_2$ solution at −125 °C that Mg^{2+} causes a redshift of the O–H stretching frequency of about 120 cm^{-1}. This shift is significantly smaller than that calculated here from the simulation. Considering the difficulties in attributing measured frequency shifts to single ion effects it is satisfying to see that the threesite model of methanol employed in the simulation describes, at least qualitatively, the effect of the ions on the intramolecular properties of methanol.

The help of Dr. M. M. Probst with the *ab initio* calculations and financial support by Deutsche Forschungsgemeinschaft and the OTKA Foundation of the Hungarian Academy of Sciences are gratefully acknowledged.

References

[1] Y. Marcus, Ion Solvation, Wiley, New York 1985.
[2] T. Radnai, E. Kálmán, and K. Pollmer, Z. Naturforsch. *39a*, 464 (1985).
[3] D. G. Montague and J. C. Dore, Mol. Phys. *57*, 1035 (1986).
[4] E. Hawlicka, G. Pálinkás, and K. Heinzinger, Chem. Phys. Lett. *154*, 255 (1989).
[5] L. M. Strauss and M. C. R. Symons, J. Chem. Soc., Faraday Trans. 1, *73*, 1796 (1977).
[6] T. L. Broadwater, T. J. Murphy, and D. F. Evans, J. Phys. Chem. *80*, 753 (1976).
[7] W. L. Jorgensen and J. Chandrasekhar, J. Am. Chem. Soc. *104*, 4584 (1982).
[8] F. Hirata and M. Levy, J. Phys. Chem. *91*, 4788 (1987).
[9] G. Pálinkás, E. Hawlicka, and K. Heinzinger, J. Phys. Chem. *91*, 4334 (1987).
[10] G. Pálinkás, Y. Tamura, E. Spohr, and K. Heinzinger, Z. Naturforsch. *43a*, 43 (1988).
[11] G. Pálinkás, E. Hawlicka, and K. Heinzinger, to be published.
[12] P. Bopp, G. Jancsó, and K. Heinzinger, Chem. Phys. Lett. *98*, 129 (1983).
[13] W. Dietz, W. O. Riede, and K. Heinzinger, Z. Naturforsch. *37a*, 1038 (1982); G. Pálinkás, T. Radnai, W. Dietz, Gy. I. Szász, and K. Heinzinger, Z. Naturforsch. *37a*, 1049 (1982); Gy. I. Szász, W. Dietz, K. Heinzinger, G. Pálinkás, and T. Radnai, Chem. Phys. Lett. *92*, 388 (1982).
[14] H. F. King and M. Dupuis, J. Comput. Phys. *21*, 144 (1976).
[15] S. Huzinaga ed., Physical Sciences Data, Vol. 16, Elsevier, Amsterdam 1984.
[16] R. M. Lees and J. G. Baker, J. Chem. Phys. *48*, 5299 (1968).
[17] A. H. Narten and A. Habenschuss, J. Chem. Phys. *80*, 3387 (1984).
[18] T. Radnai, G. Pálinkás, Gy. I. Szász, and K. Heinzinger, Z. Naturforsch. *36a*, 1076 (1981).
[19] E. Spohr, G. Pálinkás, K. Heinzinger, P. Bopp, and M. M. Probst, J. Phys. Chem. *92*, 6754 (1988).
[20] Gy. I. Szász and K. Heinzinger, J. Chem. Phys. *79*, 3467 (1983).
[21] E. Hawlicka, Z. Naturforsch. *41a*, 939 (1986).
[22] E. Hawlicka, Ber. Bunsenges. Phys. Chem. *87*, 425 (1983).
[23] K. C. Pratt and W. A. Wakeham, J. Chem. Soc. Faraday Trans. 2, *73*, 997 (1977).
[24] S. I. LaPlaca, W. C. Hamilton, B. Kamb, and A. Prakash, J. Chem. Phys. *58*, 567 (1973).
[25] S. Yamauchi and H. Kanno, Chem. Phys. Lett. *154*, 248 (1989).
[26] M. M. Probst, P. Bopp, K. Heinzinger, and B. M. Rode, Chem. Phys. Lett. *106*, 317 (1984).
[27] Y. Tamura, K. Tanaka, E. Spohr, and K. Heinzinger, Z. Naturforsch. *43a*, 1103 (1988).
[28] H. Kleeberg, G. Heinje, and W. A. P. Luck, J. Phys. Chem. *90*, 4427 (1986).

(Received on January 15th, 1991; final version on October 17th, 1991) E 7554